Physics Letters B 802 (2020) 135241

Contents lists available at ScienceDirect

Physics Letters B

www.elsevier.com/locate/physletb

Neutrino counting experiments and non-unitarity from LEP and future experiments

F.J. Escrihuela [a], L.J. Flores [b,1], O.G. Miranda [b,*]

[a] AHEP Group, Institut de Física Corpuscular – C.S.I.C., Universitat de València, Parc Cientific de Paterna, C/Catedrático José Beltrán, 2, E-46980, Paterna (València), Spain

[b] Departamento de Física, Centro de Investigación y de Estudios Avanzados del IPN, Apdo. Postal 14-740 07000, Mexico, DF, Mexico

ARTICLE INFO

Article history:
Received 6 August 2019
Received in revised form 16 January 2020
Accepted 17 January 2020
Available online 21 January 2020
Editor: W. Haxton

ABSTRACT

Non-unitarity of the neutrino mixing matrix is expected in many scenarios with physics beyond the Standard Model. Motivated by the search for deviations from unitary, we study two neutrino counting observables: the neutrino-antineutrino gamma process and the invisible Z boson decay into neutrinos. We report on new constraints for non-unitarity coming from the first of these observables. We study the potential constraints that future collider experiments will give from the invisible decay of the Z boson, that will be measured with improved precision.

1. Introduction

Particle physics is currently in an era of great progress, with new experiments [1–5] envisaged for the future. The existence of neutrino oscillations, as well as the discovery of the Higgs Boson are the main motivations for the development of new experiments that will measure the standard physics parameters with unprecedented precision, while also searching for new physics.

In the Standard Model picture, there are three active light neutrinos with an interaction governed by the $SU(2)_L \otimes U(1)_Y$ electroweak symmetry [6]. The neutrino mixing in this case is described by an unitary 3×3 matrix. If more (heavy) neutrino states exist, the corresponding mixing matrix will be bigger and it will have, at some level, a deviation from unitarity. Such picture has been studied since long time ago [7–14] and, more recently, a description in terms of a triangular parameterization has been discussed [15–18].

In the presence of such a non-unitary (NU) mixing, neutrino counting experiments at high energies will differ from the Standard Model prediction [19]. This is the case of the invisible decay width of the Z boson [20,21] and also of the $\nu\bar{\nu}\gamma$ measurements [22–32]. As far as we know, no constraints on non-unitarity have been reported from the $\nu\bar{\nu}\gamma$ process. On the opposite side, the current measurement of the invisible decay of the Z boson lies two standard deviations below the Standard Model prediction, a measurement that has already been studied with detail [33]. On the other hand, different proposals for the future generation of collider experiments are currently under development [34], such as ILC [1,35,36], FCC-ee [2,37], and CEPC [3,4,38,39]. These proposals will be running at the very high energy regime, searching for new physics and measuring the Standard Model parameters in a different energy scale. They will also test physics at relatively lower energies, in order to improve the measurements on already known observables. In particular, it is expected that the invisible Z decay width will be measured with improved precision, if compared to the current reported measurement by LEP [20,21].

In this work we study the constraints arising from the neutrino counting experiments around the Z peak, specifically using data from $\nu\bar{\nu}\gamma$ measurement. We also analyze the invisible Z decay to have a complete scenario in the same framework and study the potential of future neutrino counting experiments in the same energy regime to constraint the non-unitary parameters, and compare these perspectives with the current constraints. We will show that the perspectives in these future experiments are very promising.

In section 2, we will start the discussion by describing the non-unitarity formalism that we will use. Then, in section 3 we present the analysis used to obtain constraints on the non-unitary parameters, as well as the found results and perspectives for future experiments. Finally, in section 4 we present our conclusions.

* Corresponding author.
E-mail addresses: franesfe@alumni.uv.es (F.J. Escrihuela), jflores@fis.cinvestav.mx (L.J. Flores), omr@fis.cinvestav.mx (O.G. Miranda).
[1] Current address: Instituto de Física, Universidad Nacional Autónoma de México, A.P. 20-364, Ciudad de México 01000, México.

https://doi.org/10.1016/j.physletb.2020.135241

2. Non-unitarity, invisible Z decay and $\nu\bar{\nu}\gamma$

Non-unitarity has been subject to study for a long time [6,7,40,41]. Recent constraints can be found elsewhere [16,42], either considering only the restrictions coming from neutrino experiments, or including the ones from charged leptons. In both cases it is useful to consider the mixing matrix as describing the transformation of three light neutrinos and $n-3$ neutral heavy leptons. In this way, one can see the $U^{n\times n}$ matrix as the combination of four submatrices [43]

$$U^{n\times n} = \begin{pmatrix} N & S \\ V & T \end{pmatrix}, \tag{1}$$

with N a 3×3 submatrix in the light neutrino sector, and S the $3\times(n-3)$ submatrix that describes the mixing of the extra heavy isosinglet states.

One useful way to parameterize the non-unitarity of the mixing matrix N is the triangular parameterization [15]

$$N = N^{NP}U = \begin{pmatrix} \alpha_{11} & 0 & 0 \\ \alpha_{21} & \alpha_{22} & 0 \\ \alpha_{31} & \alpha_{32} & \alpha_{33} \end{pmatrix} U\,, \tag{2}$$

where U is the unitary PMNS mixing matrix for the standard 3×3 case and N^{NP} parameterizes the deviations from unitarity. In this way, we can encode all the parameters of the general description [6,44], for an arbitrary number of additional neutrino states, in a compact notation. In this general framework, we can describe the non-unitary phenomenology by using the three real parameters α_{11}, α_{22}, and α_{33} (all of them close to one) plus other three complex parameters $\alpha_{21}, \alpha_{31}, \alpha_{32}$ that contains extra CP violating phases and whose magnitude is small.

In what follows we will discuss two neutrino counting observables in the context of this triangular parameterization.

2.1. The invisible Z decay

In the standard unitary limit, the branching for the invisible Z decay into neutrinos will be given by [45,46],

$$\Gamma_{inv} = N_\nu \Gamma_{\nu\bar{\nu}} \tag{3}$$

with N_ν the effective number of neutrino families and [46]

$$\Gamma_{\nu\bar{\nu}} = \frac{G_F M_Z^3}{12\sqrt{2}\pi}. \tag{4}$$

Experimentally, the ratio $\Gamma_{inv}/\Gamma_{\ell\bar{\ell}}$ has been measured with greater experimental precision than Γ_{inv} alone [20,46]. Therefore, the number of light active neutrinos can be estimated from this relation, that in the Standard Model is given by [20]

$$R^0_{inv} \equiv \frac{\Gamma_{inv}}{\Gamma_{\ell\bar{\ell}}} = N_\nu \left(\frac{\Gamma_{\nu\bar{\nu}}}{\Gamma_{\ell\bar{\ell}}}\right)_{SM}, \tag{5}$$

with $N_\nu = 3$. Here, the decay rate for the Z boson into charged leptons is given by [46]

$$\Gamma_{\ell\bar{\ell}} = \frac{G_F M_Z^3 \left(g_V^{\ell\,2} + g_A^{\ell\,2}\right)}{6\sqrt{2}\pi}, \tag{6}$$

where g_V^ℓ and g_A^ℓ are the vector and axial coupling for a charged lepton ℓ:

$$g_V^\ell = T_\ell - 2Q_\ell \sin^2\theta_W\,,$$

$$g_A^\ell = T_\ell.$$

When we consider the non-unitarity formalism, applied to the invisible decay rate of the Z boson, we will find that the contribution of the three active neutrino flavors will be given by [46]

$$\Gamma_{inv} = \frac{G_F M_Z^3 \sum_{i,j} |(N^\dagger N)_{ij}|^2}{12\sqrt{2}\pi}, \tag{7}$$

that can also be expressed as

$$\Gamma_{inv} = \frac{G_F M_Z^3 \sum_{\alpha,\beta} |(NN^\dagger)_{\alpha\beta}|^2}{12\sqrt{2}\pi}. \tag{8}$$

Comparing this expression with the unitary case discussed before, we can define for the non-unitary case

$$N_\nu = \sum_{\alpha,\beta} |(NN^\dagger)_{\alpha\beta}|^2. \tag{9}$$

It is important to notice that the theoretical expression for the decay rate will be affected by non-unitarity with several corrections. However, we must notice that there is another correction due to the definition of G_F. In order to introduce this correction, we can write the equivalent expression to Eq. (5) for the non-unitary case. For this purpose, we start by considering that, from muon decay, a non-unitary mixing will affect the value of the Fermi constant to be [7,41,47]

$$G_F = \frac{G_\mu}{\sqrt{\sum_{ij} |N_{\mu i}|^2 |N_{ej}|^2}} = \frac{G_\mu}{\sqrt{\alpha_{11}^2(\alpha_{22}^2 + |\alpha_{21}|^2)}}\,. \tag{10}$$

This correction cancels out in the ratio, R^0_{inv}, but can propagate to other observables, such as the weak mixing angle [42]

$$\sin^2\theta_W = \frac{1}{2}\left(1 - \sqrt{1 - \frac{2\sqrt{2}\alpha\pi}{G_\mu M_Z^2}\sqrt{\alpha_{11}^2(\alpha_{22}^2 + |\alpha_{21}|^2)}}\right). \tag{11}$$

From Eqs. (9) and (6), we can get an expression for the ratio in the non-unitary case:

$$R^0_{inv} = \frac{\sum_{\alpha,\beta} |(NN^\dagger)_{\alpha\beta}|^2}{2(g_V^{\ell\,2} + g_A^{\ell\,2})}. \tag{12}$$

Let us notice that the deviation from unitarity, introduced by the parameters α_{ij}, appears explicitly in the numerator through $|(NN^\dagger)_{\alpha\beta}|^2$, but also implicitly in the denominator via g_V^ℓ, because it contains the expression for the weak mixing given in Eq. (11). The explicit form for the numerator in the previous formula will be

$$\begin{aligned}\sum_{\alpha,\beta} |(NN^\dagger)_{\alpha\beta}|^2 = {} & \alpha_{11}^4 + \alpha_{22}^4 + \alpha_{33}^4 + |\alpha_{21}|^4 + |\alpha_{31}|^4 + |\alpha_{32}|^4 \\ & + 2\alpha_{22}^2|\alpha_{21}|^2 + 2\alpha_{33}^2(|\alpha_{31}|^2 + |\alpha_{32}|^2) \\ & + 2|\alpha_{31}|^2|\alpha_{32}|^2 \\ & + 2\alpha_{11}^2(|\alpha_{21}|^2 + |\alpha_{31}|^2) + 2|\alpha_{21}\alpha_{31}^* + \alpha_{22}\alpha_{32}^*|^2.\end{aligned} \tag{13}$$

If we neglect terms including third order or higher on off-diagonal parameters ($\alpha_{ij}\ i \neq j$), we obtain the following reduced expression:

$$\begin{aligned}\sum_{\alpha,\beta} |(NN^\dagger)_{\alpha\beta}|^2 = {} & \alpha_{11}^4 + \alpha_{22}^4 + \alpha_{33}^4 + 2\alpha_{11}^2(|\alpha_{21}|^2 + |\alpha_{31}|^2) \\ & + 2\alpha_{22}^2(|\alpha_{21}|^2 + |\alpha_{32}|^2) \\ & + 2\alpha_{33}^2(|\alpha_{31}|^2 + |\alpha_{32}|^2)\,.\end{aligned}$$

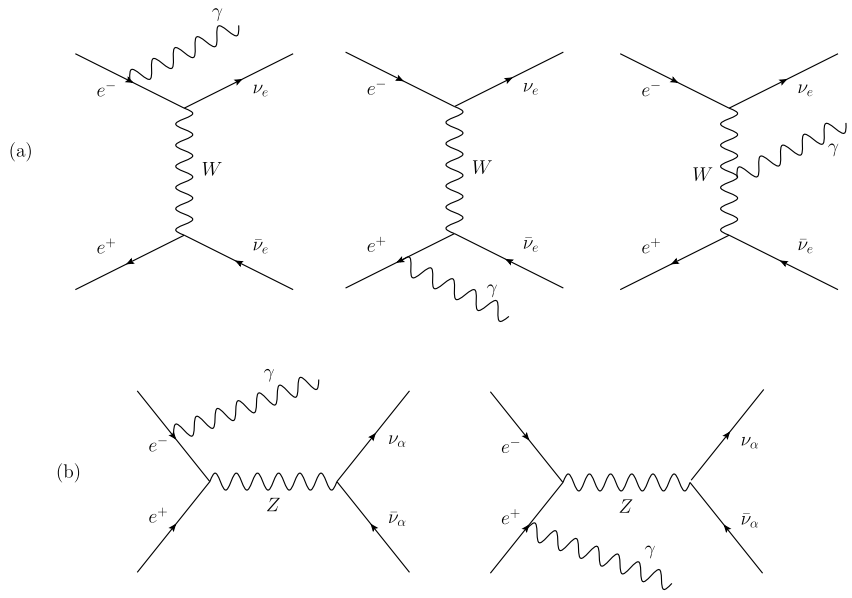

Fig. 1. Contributions to the $e^-e^+ \to \nu\bar{\nu}\gamma$ process at tree level, from the W (a) and Z (b) bosons.

Different constraints for the α_{ij} parameters show that N^{NP} is close to an identity matrix.

Besides, the precision of the measurements under consideration makes necessary to introduce radiative corrections. In the $\overline{MS}$ scheme, the weak mixing angle takes the form [46]

$$\hat{s}_Z = \frac{A_0}{M_W(1-\Delta\hat{r}_W)^{1/2}}, \tag{14}$$

where, in the non-unitary case, A_0 is given by

$$A_0 = \left(\frac{\pi\alpha}{\sqrt{2}G_F}\right)^{1/2} = \left(\frac{\pi\alpha\sqrt{\alpha_{11}^2(\alpha_{22}^2+|\alpha_{21}|^2)}}{\sqrt{2}G_\mu}\right)^{1/2}, \tag{15}$$

$\Delta\hat{r}_W$ introduces the radiative corrections, and M_W is the mass of the W boson. According to PDG [46], the values of the relevant parameters are:

$$M_W = 80.379 \pm 0.012\ \text{GeV/c}^2\,, \tag{16}$$
$$\Delta\hat{r}_W = 0.06916 \pm 0.00008\,, \tag{17}$$
$$\alpha = (7.2973525664 \pm 0.0000000017) \times 10^{-3}\,, \tag{18}$$
$$G_\mu = (1.1663787 \pm 0.0000006) \times 10^{-5}\ \text{GeV}^2 \tag{19}$$
$$\hat{s}_Z^2 = 0.23122 \pm 0.00003\,. \tag{20}$$

For measurements at energies around the Z peak it is common to use the effective weak mixing angle $\bar{s}_l^2$ instead of the $\overline{MS}$ scheme; both quantities are related through [46] $\bar{s}_l^2 = \hat{s}_Z^2 + 0.00032$.

Now we can turn now our attention to the comparison with the experimental results to obtain constraints and future perspectives for the NU parameters. However, before entering into this discussion we will also discuss another neutrino counting observable.

2.2. The process $e^-e^+ \to \nu\bar{\nu}\gamma$

Another process that was also measured at LEP, and allows for a neutrino counting, is the single photon production with a neutrino-antineutrino pair [22–32]. In this subsection we compute the expression for this observable in the NU case.

The differential cross section for the single photon production from electron-positron annihilation, $e^+e^- \to \nu\bar{\nu}\gamma$, can be written in terms of the radiator function $H(x, y; s)$ and the "reduced" cross section for the process $e^+e^- \to \nu\bar{\nu}$, σ_0, as [48–50]:

$$\frac{d^2\sigma}{dx\,dy} = H(x, y; s)\,\sigma_0(s(1-x)). \tag{21}$$

The radiator function is defined by

$$H(x, y; s) = \frac{2\alpha}{\pi}\frac{\left[(1-\frac{1}{2}x)^2 + \frac{1}{4}x^2y^2\right]}{x(1-y^2)}, \tag{22}$$

with

$$x = 2E_\gamma/\sqrt{s}, \quad y = \cos\theta_\gamma, \tag{23}$$

and σ_0, the "reduced" cross section for the process $e^+e^- \to \nu\bar{\nu}$ is given by

$$\sigma_0(s) = \sigma_W(s) + \sigma_Z(s) + \sigma_{W-Z}(s),$$
$$\sigma_0(s) = \frac{G_F^2 s}{12\pi}\left[2 + \frac{N_\nu(g_V^2+g_A^2)}{(1-s/M_Z^2)^2+\Gamma_Z^2/M_Z^2} + \frac{2(g_V+g_A)(1-s/M_Z^2)}{(1-s/M_Z^2)^2+\Gamma_Z^2/M_Z^2}\right]. \tag{24}$$

The three terms in Eq. (24) come from the contribution of the W, the Z boson, and their interference, as can be seen in the Feynman diagrams in Fig. 1.

For energies above the Z resonance, finite distance effects on the W propagator need to be considered. These effects are taken into account by the following substitution [32,49,50]:

$$\sigma_W(s) \to \sigma_W(s)F_W(s/M_W^2),$$
$$\sigma_{W-Z}(s) \to \sigma_{W-Z}(s)F_{W-Z}(s/M_W^2), \tag{25}$$

where

$$F_W(z) = \frac{3}{z^3}\left[-2(z+1)\log(z+1) + z(z+2)\right],$$
$$F_{W-Z}(z) = \frac{3}{z^3}\left[(z+1)^2\log(z+1) - z(\tfrac{3}{2}z+1)\right]. \tag{26}$$

It is important to notice that the expression in Eq. (24), including the corrections from Eq. (25), is equivalent to the widely used expression:

$$\sigma_0(s) = \frac{N_\nu G_F^2}{6\pi} M_Z^4 (g_R^2 + g_L^2) \frac{s}{\left[\left(s - M_Z^2\right)^2 + (M_Z\Gamma_Z)^2\right]} + \frac{G_F^2}{\pi} M_W^2 \left\{ \frac{s + 2M_W^2}{2s} - \frac{M_W^2}{s}\left(\frac{s + M_W^2}{s}\right)\log\left(\frac{s + M_W^2}{M_W^2}\right) - g_L \frac{M_Z^2(s - M_Z^2)}{\left(s - M_Z^2\right)^2 + (M_Z\Gamma_Z)^2} \times \left[\frac{\left(s + M_W^2\right)^2}{s^2}\log\left(\frac{s + M_W^2}{M_W^2}\right) - \frac{M_W^2}{s} - \frac{3}{2}\right]\right\}. \quad (27)$$

Nevertheless, we will continue using Eq. (24), since the introduction of the non-unitarity effects can be made in a more transparent way.

From Eq. (21), the total cross section is

$$\sigma(s) = \int_{x_{\min}}^{1} dx \int_{-\cos\theta_{\min}}^{\cos\theta_{\min}} dy H(x, y; s)\, \sigma_0(s(1 - x)). \quad (28)$$

If we now examine this process in a non-unitary mixing framework, it is almost straightforward to obtain the non-unitarity effects in the reduced cross section:

$$\sigma_0^{NU}(s) = \sum_{i,j} |N_{ei}|^2 |N_{ej}|^2\, \sigma_W(s) F_W(s/M_W^2) + \sum_{\alpha,\beta} |(NN^\dagger)_{\alpha\beta}|^2\, \sigma_Z(s) + \sum_{i,j} |N_{ei}|^2 |N_{ej}|^2\, \sigma_{W-Z}(s) F_{W-Z}(s/M_W^2). \quad (29)$$

These corrections can be seen in Fig. 1: for the W contribution (a), each neutrino line contributes with a term U_{ei} in the scattering amplitude, while for the Z contribution (b), the provided correction is of the form $U_{\alpha i}$. Since the mixing is non-unitary, flavor-changing neutral currents are allowed, hence the sum must be given over different flavors in the second term of Eq. (29).

Writing Eq. (29) explicitly, we will have

$$\sigma_0^{NU}(s) = \frac{G_F^2 s}{12\pi}\left[2\sum_{i,j} |N_{ei}|^2 |N_{ej}|^2 + \sum_{\alpha,\beta} |(NN^\dagger)_{\alpha\beta}|^2 \frac{(g_V^2 + g_A^2)}{(1 - s/M_Z^2)^2 + \Gamma_Z^2/M_Z^2} + \sum_{i,j} |N_{ei}|^2 |N_{ej}|^2 \frac{2(g_V + g_A)(1 - s/M_Z^2)}{(1 - s/M_Z^2)^2 + \Gamma_Z^2/M_Z^2}\right]. \quad (30)$$

Additionally, as discussed in the previous subsection, there will be NU corrections to G_F and $\sin^2\theta_W$ as described in Eqs. (10) and (11) respectively. Finally, it should be noticed that in the last two terms of Eq. (29), the decay width, Γ_Z, appears in the denominator. Since we are considering the NU case, we must also introduce the corresponding corrections. The total Z decay width can be calculated as [45,46]

$$\Gamma_Z = \Gamma_{\text{inv}} + \Gamma_{\ell\ell} + \Gamma_{\text{had}} \quad (31)$$

and the non-unitary correction will appear through the Γ_{inv} contribution, as it had been computed in the previous subsection, and we will have:

$$\Gamma_Z = \frac{G_F M_Z^3}{12\sqrt{2}\pi} \sum_{\alpha,\beta} |(NN^\dagger)_{\alpha\beta}|^2 + \Gamma_{\ell\ell} + \Gamma_{\text{had}}. \quad (32)$$

Now that we have introduced the theoretical expressions for the two neutrino counting observables with the formalism for the non-unitary case, in the triangular parameterization, we will discuss the corresponding current constraints and future perspectives for these two cases.

3. Experimental tests

3.1. The process $e^-e^+ \to \nu\bar{\nu}\gamma$

To obtain constraints for the NU case from the process $e^-e^+ \to \nu\bar{\nu}\gamma$, we use the reported measurements from the ALEPH [24], DELPHI [25], L3 [26–28], and OPAL [29–31] collaborations. They are listed in Table 1. The center of mass energy for each run is listed in the first column. The background subtracted measured and Monte Carlo cross sections are given in columns two and three, respectively. The number of observed events after background subtraction are given in column four, while the efficiency corresponds to column five. Lastly, the kinematical cuts for the outgoing photon energy and angle are reported in the last two columns. For these cuts, $x_T = x\sin\theta_\gamma$ (with $x = E_\gamma/E_{\text{beam}}$), while $y = \cos\theta_\gamma$.

In order to make our analysis, we have computed the cross section from Eqs. (28) and (30), with the integration limits taken according to the last two columns of Table 1. Although we have a good agreement in our integration with many of the reported Monte Carlo simulations, there are some exceptions due, we believe, to our lack of knowledge of each experimental setup. Instead of excluding any experimental value, we have included a normalization error in our analysis, with a 10% uncertainty. Once we have obtained this expression, we have compared our theoretical expectation for the NU case with the experimental results of Table 1 through a χ^2 analysis.

Our result for the non-unitary parameter α_{11} is shown in Fig. 2, for each experiment separately, and for a combination of all of them. In this analysis, we have considered any other NU parameter as equal to the Standard case, that is, $\alpha_{22}^2 = \alpha_{33}^2 = 1$ and $\alpha_{21}^2 = \alpha_{31}^2 = \alpha_{32}^2 = 0$. We have chosen this parameter because diagonal parameters α_{ii} give the main contribution for deviations from unitarity. Besides, any diagonal parameter contributes on equal footing and, therefore, our constrain can be equally applied to α_{22} or α_{33}. As it can be seen, it is possible to restrict the α_{11} NU parameter, and the constraint at 90% CL is given by

$$\alpha_{11} > 0.9794, \quad 1 - \alpha_{11} < 0.0206. \quad (33)$$

To our knowledge, this is the first time that a constraint for NU is reported using this observable and it is possible to see that the limits are competitive.

3.2. The invisible Z decay

We now turn our attention to the particular case of the Z decay into neutrinos. This process has already been measured by LEP [20,21] and future experiments [1–4,34–39] can improve the measurement of this important observable. Previous works have already reported constraints on NU parameters using this observable for a

Table 1
Summary from the ALEPH [22–24], DELPHI [25], L3 [26–28], and OPAL [29–31] collaboration experimental data, collected above the W^+W^- production threshold.

		$\sqrt{s}$ (GeV)	σ^{mes} (pb)	σ^{MC} (pb)	N_{obs}	ϵ(%)	E_γ (GeV)	$\lvert y\rvert$
ALEPH	[22]	161	5.3 ± 0.83	5.81 ± 0.03	41	70	$x_T \geq 0.075$	≤ 0.95
		172	4.7 ± 0.83	4.85 ± 0.04	36	72	$x_T \geq 0.075$	≤ 0.95
	[23]	183	4.32 ± 0.34	4.15 ± 0.03	195	77	$x_T \geq 0.075$	≤ 0.95
	[24]	189	3.43 ± 0.17	3.48 ± 0.05	484	81.5	$x_T \geq 0.075$	≤ 0.95
		192	3.47 ± 0.40	3.23 ± 0.05	81			
		196	3.03 ± 0.23	3.26 ± 0.05	197			
		200	3.23 ± 0.22	3.12 ± 0.05	231			
		202	2.99 ± 0.29	3.07 ± 0.05	110			
		205	2.84 ± 0.22	2.93 ± 0.05	182			
		207	2.67 ± 0.17	2.80 ± 0.05	292			
DELPHI	[25]	189	1.80 ± 0.20	1.97	146	51	$x \geq 0.06$	≤ 0.7
		183	2.33 ± 0.36	2.08	65	54	$x \geq 0.02$	≤ 0.85
		189	1.89 ± 0.22	1.94	155	50	$x \leq 0.9$	≤ 0.98
L3	[26]	161	6.75 ± 0.93	6.26 ± 0.12	57	80.5	≥ 10 and	≤ 0.73 and
		172	6.12 ± 0.90	5.61 ± 0.10	49	80.7	$E_T \geq 6$	0.80-0.97
	[27]	183	5.36 ± 0.40	5.62 ± 0.10	195	65.4	≥ 5 and	≤ 0.73 and
	[28]	189	5.25 ± 0.23	5.29 ± 0.06	572	60.8	$E_T \geq 5$	0.80-0.97
OPAL	[29]	130	10.0 ± 2.34	13.48 ± 0.22	19	81.6	$x_T > 0.05$ and	≤ 0.82 and
		136	16.3 ± 2.89	11.30 ± 0.20	34	79.7	$x_T > 0.1$	≤ 0.966
	[30]	130	11.6 ± 2.53	14.26 ± 0.06	21	77	$x_T > 0.05$	≤ 0.966
		136	14.9 ± 2.45	11.95 ± 0.07	39	77.5		
	[29]	161	5.30 ± 0.83	6.49 ± 0.08	40	75.2	$x_T > 0.05$ and	≤ 0.82 and
		172	5.50 ± 0.83	5.53 ± 0.08	45	77.9	$x_T > 0.1$	≤ 0.966
	[30]	183	4.71 ± 0.38	4.98 ± 0.02	191	74.2	$x_T > 0.05$	≤ 0.966
	[31]	189	4.35 ± 0.19	4.66 ± 0.03	643	82.1	$x_T > 0.05$	≤ 0.966

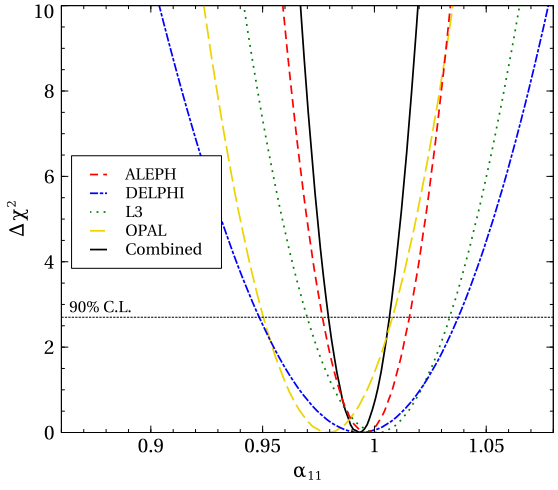

Fig. 2. Bounds on the NU parameter α_{11} from the process $e^-e^+ \to \nu\bar{\nu}\gamma$, using the ALEPH, DELPHI, L3, and OPAL reported results.

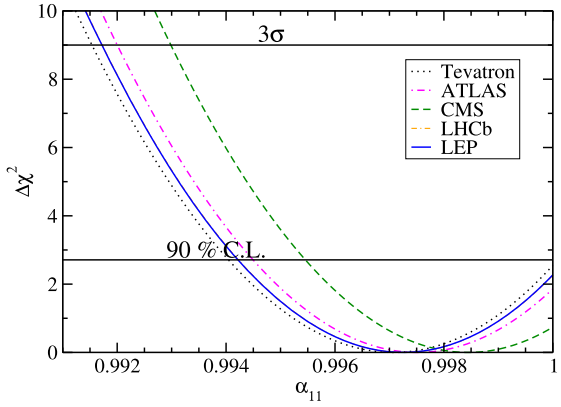

Fig. 3. Restrictions for α_{11} from the invisible decay of the Z boson, depending on the value of the effective weak mixing angle, $\bar{s}_l^2$. We consider the measurements on $\bar{s}_l^2$ coming from different experiments.

combined analysis from different measurements [42,51–53]. Here we focus on this particular parameter using the specific triangular parameterization and making more emphasis in the perspectives from future experimental proposals.

Before analyzing the invisible decay constraints on NU, it is important to remember from the previous section that the NU case will affect the theoretical prediction of different parameters, such as G_F and $\sin^2\theta_W$ (Eqs. (10) and (11) respectively). Perhaps the most important observable for our discussion is the value of the weak mixing angle that, at the relevant energy, differs up to three standard deviations depending on the experiment that measures it. Its impact is illustrated in Fig. 3, where we show the χ^2 curve for this observable as a function of the α_{11} parameter. In this figure, besides considering the LEP [20,21] measurement for the weak mixing angle, we also show how this constraint changes if we consider other measurements for the weak mixing angle. That is the case of the Tevatron [54–57], Atlas [58], LHCb [59] and CMS [60] result. It is possible to notice that the evaluation of this fundamental quantity of the Standard Model still can have an impact on the non-unitarity constraints. As in the previous subsection, for this plot we have only considered α_{11} as different from one and all other non-unitary parameters as equal to the standard case, that is, $\alpha_{22}^2 = \alpha_{33}^2 = 1$ and $\alpha_{21}^2 = \alpha_{31}^2 = \alpha_{32}^2 = 0$.

Table 2
Expected uncertainties on N_ν and $\sin^2\theta_{eff}$ for different experimental proposals. Notice that for LEP we quote the present experimental values, whereas for CEPC, FCC-ee, and ILC we show future estimations.

	LEP [20]	CEPC [4]	FCC-ee [2]	ILC [1]
$\sigma(N_\nu)[10^{-3}]$	8.0	3.0	4.0	4.0
$\sigma(\sin^2\theta_{eff})[10^{-4}]$	1.6	0.23	0.01	0.1

Table 3
Test values for the invisible ratio R^0_{inv} used in the present work. We quote the expected uncertainty coming from future experiments.

	CEPC		
R^0_{inv}	5.9430 ± 0.0065	5.9671 ± 0.0065	5.9801 ± 0.0065
	FCC-ee/ILC		
R^0_{inv}	5.9430 ± 0.0083	5.9671 ± 0.0083	5.9801 ± 0.0083

Provided that we have a precise measurement of the weak mixing angle, we can return to the computation of constraints on NU from current and future experimental proposals that will improve the measurements of different observables, such as the number of neutrinos, N_ν, or the effective value of the weak mixing angle, $\sin^2\theta_{eff}$. We show their sensitivity in Table 2.

In order to estimate the sensitivity of the future experiments we will consider again the ratio given by Eq. (5). In particular, the uncertainty of R^0_{inv} is calculated from

$$\sigma^2(R^0_{inv}) = \left(\frac{\Gamma_{\nu\bar{\nu}}}{\Gamma_{l\bar{l}}}\right)^2_{SM} \sigma^2(N_\nu) + (N_\nu)^2\,\sigma^2\left(\frac{\Gamma_{\nu\bar{\nu}}}{\Gamma_{l\bar{l}}}\right)_{SM},$$

where $\sigma\left(\frac{\Gamma_{\nu\bar{\nu}}}{\Gamma_{l\bar{l}}}\right)_{SM} = 0.00083$ [20] and $\sigma(N_\nu)$ is given in Table 2. With this hypothesis we obtain the results shown in Table 3.

Within this framework, it is possible to obtain an idea of the future sensitivity of these experiments on the NU parameters. A forecast for this sensitivity can be computed considering three different cases of a future measurement of the ratio R^0_{inv}:

- The experimental value reported at [20], $R^0_{inv} = 5.9430$.
- The theoretical value calculated from the effective weak mixing angle including radiative corrections [61], $R^0_{inv} = 5.9671$.
- A value two standard deviations (of CEPC) above of the previous value, $R^0_{inv} = 5.9801$.

To consider these futuristic scenarios, it takes into account the possible non-standard result where the effective number of neutrinos is smaller than three. Besides, it also considers the less expected case where a future experiment might have a statistical fluctuation, and measures a value above the SM prediction. For these three cases, we perform a χ^2 analysis in order to have a forecast of the future expected sensitivity, considering the following two scenarios:

- Firstly, we consider that α_{11} is the only parameter different from the standard case. The χ^2 fit is made with the errors already discussed for each experiment. The results are compiled in Fig. 4.
- Secondly, we let α_{11}, α_{13} and α_{33} to vary freely, while fulfilling the Cauchy-Schwarz condition:

$$|\alpha_{ij}| \leq \sqrt{(1-\alpha^2_{ii})\,(1-\alpha^2_{jj})}\,. \tag{34}$$

The other NU parameters are set to their SM value. The results obtained are shown in Fig. 5. Notice that we have considered only α_{33} and α_{31} different from zero, since very similar results will be obtained with α_{22} and α_{21}.

We summarize the expected accuracy for both cases in Table 4. We can see from these results that future collider experiments could give a constraint on the diagonal non-unitary parameter that will be stronger than the current global limits [16,18,42], that constraints α_{11} at the level of 0.999 or below as we see in Table 5. It is also interesting to notice what would be the constraint in the case of a measurement different from the SM prediction; as illustrated in the same Table 4 the future experiments under discussion will have the potential to show the evidence of new physics through a non-unitarity of the neutrino mixing-matrix.

4. Conclusions

We have reviewed the measurements for neutrino counting observables close to the Z peak and reported a new analysis for the non-unitary formalism for the case of the $\nu\bar{\nu}\gamma$ process. The corresponding constraints have been introduced in this work and we have shown that they are competitive with other current constraints. As far as we know, this is the first time this analysis is done. We have used the triangular parameterization to perform this analysis.

We have also analyzed the invisible Z decay into neutrinos, in the same triangular parameterization. In this case we have focused in the importance of a precise determination of the weak mixing angle and in the perspectives to improve current constraints by using future collider experiments, that are expected to be constructed as a continuation of the precision program for particle

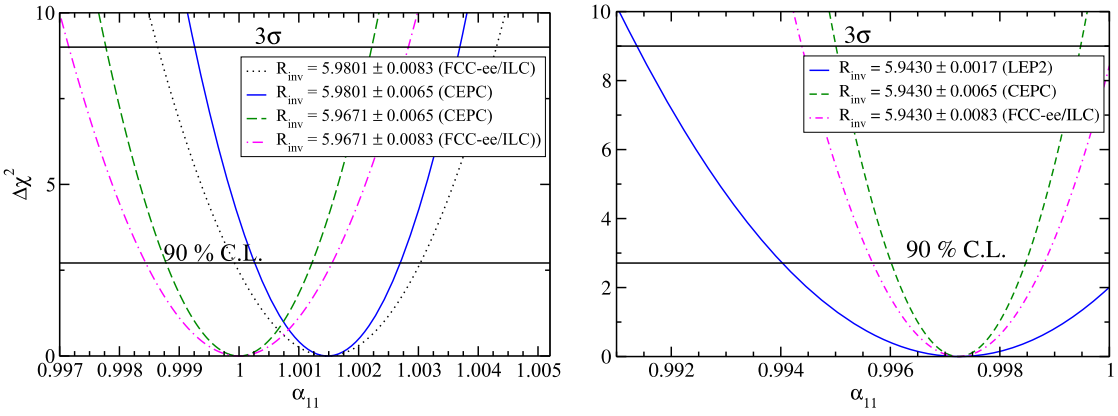

Fig. 4. Restrictions for α_{11} from the invisible decay of the Z boson, for the future proposals CEPC, FCC-ee and ILC experiments. We have considered different possible central values to illustrate the constraints to be obtained.

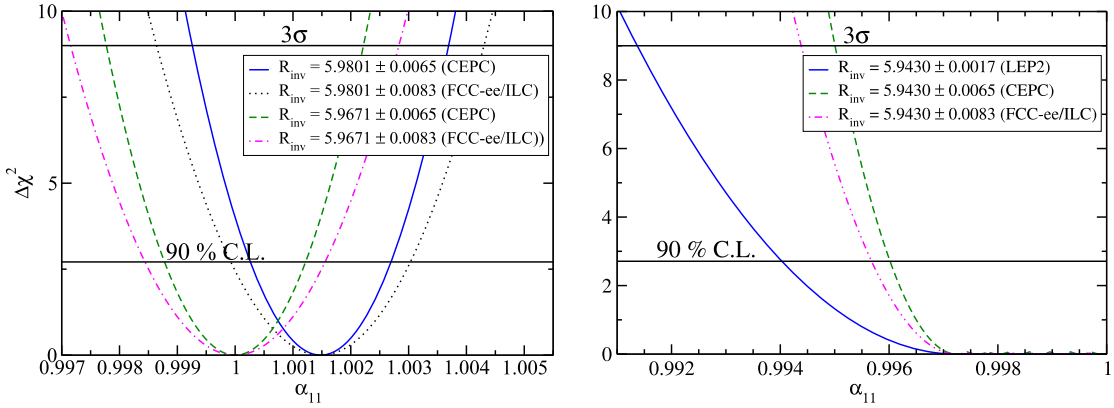

Fig. 5. Restrictions for α_{11} from the invisible decay of the Z boson for the future CEPC, FCC-ee and ILC experiments. Different central values have been used as a test to illustrate the possible constraints. For this case, we have considered α_{33} and α_{31} as free parameters in the fit (fulfilling the Cauchy-Schwartz condition).

Table 4
Allowed values for α_{11} at 90% C.L., considering present experimental values and future proposals from CEPC, FCC-ee and ILC experiments. We consider either the case when any NU parameter other than α_{11} is in the unitary limit and also when α_{31} and α_{33} are allowed to vary, fulfilling the Cauchy-Schwartz condition.

Experiment	R^0_{inv}	α_{11}	α_{11} (α_{31} and α_{33} free)
Current	5.9430	$0.99403 < \alpha_{11}$	$0.99403 < \alpha_{11}$
CEPC	5.9430	$0.99602 < \alpha_{11} < 0.99847$	$0.99602 < \alpha_{11}$
FCC-ee/ILC	5.9430	$0.99568 < \alpha_{11} < 0.99881$	$0.99568 < \alpha_{11}$
CEPC	5.9671	$0.99879 < \alpha_{11} < 1.00123$	$0.99879 < \alpha_{11} < 1.00123$
FCC-ee/ILC	5.9671	$0.99844 < \alpha_{11} < 1.00156$	$0.99845 < \alpha_{11} < 1.00157$
CEPC	5.9801	$1.00026 < \alpha_{11} < 1.00269$	$1.00027 < \alpha_{11} < 1.00270$
FCC-ee/ILC	5.9801	$0.99993 < \alpha_{11}; < 1.00305$	$0.99994 < \alpha_{11} < 1.00304$

Table 5
Current bounds on non-unitary α_{11} parameters coming from [16,18,42].

Current bounds		
α_{11} (90% C.L.) [16]		α_{11} (2σ) [18,42]
One parameter	All parameters	
$\alpha_{11} > 0.98000$	$\alpha_{11} > 0.96000$	$\alpha_{11} > 0.99875$

physics. They will allow to obtain better restrictions to new physics from several processes at different energy regimes. For this purpose, we have focused in the invisible decay width in the Z peak, that will be measured in the first stages of the future collider experiments ILC, FCC-ee and CEPC.

We have shown that any of these experiments will have enough sensitivity to improve the current constraint on non-unitarity. We have focused especially in the diagonal parameter α_{11}. To obtain this result we have used different test values. In particular, for a measurement as low as the current LEP central value, future experiments will give a positive signal for non-unitarity at 90% C.L., while a future measurement in accordance with the Standard model prediction will restrict the limit for α_{11} to be bigger that 0.999, that is, a precision at the level of 10^{-3}. It is also important to notice that, as can be seen from Eq. (13), the Z decay measurement will mainly restrict the sum of the three diagonal parameters: $\sum_i \alpha_{ii}$ and, therefore, in a combined analysis, this measurement will help to restrict any of the diagonal parameters.

Acknowledgements

This work was supported by the CONACYT grant A1-S-23238 and SNI (Mexico). LJF also thanks the CONACYT for the grant of Ayudante de investigador (EXP. AYTE. 16959) and for a posdoctoral CONACYT grant.

References

[1] H. Baer, T. Barklow, K. Fujii, Y. Gao, A. Hoang, S. Kanemura, J. List, H.E. Logan, A. Nomerotski, M. Perelstein, et al., arXiv:1306.6352, 2013.
[2] M. Bicer, et al., TLEP Design Study Working Group, J. High Energy Phys. 01 (2014) 164, arXiv:1308.6176.
[3] M. Dong, et al., CEPC Study Group, 2018, arXiv:1811.10545.
[4] M. Ahmad, et al., TLEP Design Study Working Group, Report Number: IHEP-CEPC-DR-2015-01 2015, unpublished.
[5] M.J. Boland, et al., CLICdp, CLIC, arXiv:1608.07537, 2016.
[6] J. Schechter, J.W.F. Valle, Phys. Rev. D 22 (1980) 2227.
[7] E. Nardi, E. Roulet, D. Tommasini, Phys. Lett. B 327 (1994) 319, arXiv:hep-ph/9402224.
[8] S. Antusch, C. Biggio, E. Fernandez-Martinez, M.B. Gavela, J. Lopez-Pavon, J. High Energy Phys. 10 (2006) 084, arXiv:hep-ph/0607020.
[9] A.Yu. Smirnov, R. Zukanovich Funchal, Phys. Rev. D 74 (2006) 013001, arXiv:hep-ph/0603009.
[10] P.S.B. Dev, R.N. Mohapatra, Phys. Rev. D 81 (2010) 013001, arXiv:0910.3924.
[11] T. Ohlsson, C. Popa, H. Zhang, Phys. Lett. B 692 (2010) 257, arXiv:1007.0106.
[12] E. Akhmedov, A. Kartavtsev, M. Lindner, L. Michaels, J. Smirnov, J. High Energy Phys. 05 (2013) 081, arXiv:1302.1872.
[13] A. de Gouvêa, A. Kobach, Phys. Rev. D 93 (2016) 033005, arXiv:1511.00683.
[14] S. Antusch, O. Fischer, Int. J. Mod. Phys. A 31 (2016) 1644006, Int. J. Mod. Phys. A 83 (2017), arXiv:1604.00208.
[15] F.J. Escrihuela, D.V. Forero, O.G. Miranda, M. Tortola, J.W.F. Valle, Phys. Rev. D 92 (2015) 053009, Erratum: Phys. Rev. D 93 (11) (2016) 119905, arXiv:1503.08879.
[16] F.J. Escrihuela, D.V. Forero, O.G. Miranda, M. Tórtola, J.W.F. Valle, New J. Phys. 19 (2017) 093005, arXiv:1612.07377.
[17] O.G. Miranda, J.W.F. Valle, Nucl. Phys. B 908 (2016) 436, arXiv:1602.00864.
[18] M. Blennow, P. Coloma, E. Fernandez-Martinez, J. Hernandez-Garcia, J. Lopez-Pavon, J. High Energy Phys. 04 (2017) 153, arXiv:1609.08637.
[19] M.C. Gonzalez-Garcia, A. Santamaria, J.W.F. Valle, Nucl. Phys. B 342 (1990) 108.
[20] S. Schael, et al., SLD Electroweak Group, DELPHI, ALEPH, SLD, SLD Heavy Flavour Group, OPAL, LEP Electroweak Working Group, L3, Phys. Rep. 427 (2006) 257, arXiv:hep-ex/0509008.
[21] S. Schael, et al., DELPHI, OPAL, LEP Electroweak, ALEPH, L3, Phys. Rep. 532 (2013) 119, arXiv:1302.3415.
[22] R. Barate, et al., ALEPH, Phys. Lett. B 420 (1998) 127, arXiv:hep-ex/9710009.
[23] R. Barate, et al., ALEPH, Phys. Lett. B 429 (1998) 201.

[24] A. Heister, et al., ALEPH, Eur. Phys. J. C 28 (2003) 1.
[25] P. Abreu, et al., DELPHI, Eur. Phys. J. C 17 (2000) 53, arXiv:hep-ex/0103044.
[26] M. Acciarri, et al., L3, Phys. Lett. B 415 (1997) 299.
[27] M. Acciarri, et al., L3, Phys. Lett. B 444 (1998) 503.
[28] M. Acciarri, et al., L3, Phys. Lett. B 470 (1999) 268, arXiv:hep-ex/9910009.
[29] K. Ackerstaff, et al., OPAL, Eur. Phys. J. C 2 (1998) 607, arXiv:hep-ex/9801024.
[30] G. Abbiendi, et al., OPAL, Eur. Phys. J. C 8 (1999) 23, arXiv:hep-ex/9810021.
[31] G. Abbiendi, et al., OPAL, Eur. Phys. J. C 18 (2000) 253, arXiv:hep-ex/0005002.
[32] M. Hirsch, E. Nardi, D. Restrepo, Phys. Rev. D 67 (2003) 033005, arXiv:hep-ph/0210137.
[33] M. Carena, A. de Gouvea, A. Freitas, M. Schmitt, Phys. Rev. D 68 (2003) 113007, arXiv:hep-ph/0308053.
[34] J. Fan, M. Reece, L.-T. Wang, J. High Energy Phys. 09 (2015) 196, arXiv:1411.1054.
[35] M. Baak, et al., in: Proceedings, 2013 Community Summer Study on the Future of U.S. Particle Physics: Snowmass on the Mississippi (CSS2013), Minneapolis, MN, USA, July 29–August 6, 2013, 2013, arXiv:1310.6708, http://www.slac.stanford.edu/econf/C1307292/docs/EnergyFrontier/Electroweak-19.pdf.
[36] S. Banerjee, P.S.B. Dev, A. Ibarra, T. Mandal, M. Mitra, Phys. Rev. D 92 (2015) 075002, arXiv:1503.05491.
[37] A. Blondel, E. Graverini, N. Serra, M. Shaposhnikov, FCC-ee study Team, Nucl. Part. Phys. Proc. 273–275 (2016) 1883, arXiv:1411.5230.
[38] W. Liao, X.-H. Wu, Phys. Rev. D 97 (2018) 055005, arXiv:1710.09266.
[39] H. Liang, M. Ruan, Int. J. Mod. Phys. Conf. Ser. 46 (2018) 1860086.
[40] M. Gronau, C.N. Leung, J.L. Rosner, Phys. Rev. D 29 (1984) 2539.
[41] A. Atre, T. Han, S. Pascoli, B. Zhang, J. High Energy Phys. 05 (2009) 030, arXiv:0901.3589.
[42] E. Fernandez-Martinez, J. Hernandez-Garcia, J. Lopez-Pavon, J. High Energy Phys. 08 (2016) 033, arXiv:1605.08774.
[43] H. Hettmansperger, M. Lindner, W. Rodejohann, J. High Energy Phys. 04 (2011) 123, arXiv:1102.3432.
[44] W. Rodejohann, J.W.F. Valle, Phys. Rev. D 84 (2011) 073011, arXiv:1108.3484.
[45] E.K. Akhmedov, in: Proceedings, Summer School in Particle Physics, Trieste, Italy, June 21–July 9, 1999, 1999, pp. 103–164, arXiv:hep-ph/0001264.
[46] M. Tanabashi, et al., Particle Data Group, Phys. Rev. D 98 (2018) 030001.
[47] P. Langacker, D. London, Phys. Rev. D 38 (1988) 886.
[48] O. Nicrosini, L. Trentadue, Nucl. Phys. B 318 (1989) 1.
[49] J. Barranco, O.G. Miranda, C.A. Moura, J.W.F. Valle, Phys. Rev. D 77 (2008) 093014, arXiv:0711.0698.
[50] Z. Berezhiani, A. Rossi, Phys. Lett. B 535 (2002) 207, arXiv:hep-ph/0111137.
[51] S. Antusch, O. Fischer, J. High Energy Phys. 10 (2014) 094, arXiv:1407.6607.
[52] S. Antusch, O. Fischer, J. High Energy Phys. 05 (2015) 053, arXiv:1502.05915.
[53] O. Fischer, S. Antusch, PoS DIS 2017 (2018) 090, arXiv:1709.00880.
[54] V.M. Abazov, et al., D0, Phys. Rev. D 84 (2011) 012007, arXiv:1104.4590.
[55] D. Acosta, et al., CDF, Phys. Rev. D 71 (2005) 052002, arXiv:hep-ex/0411059.
[56] T.A. Aaltonen, et al., CDF, D0, Phys. Rev. D 88 (2013) 052018, arXiv:1307.7627.
[57] Tevatron Electroweak Working Group, arXiv:1003.2826 [hep-ex].
[58] G. Aad, et al., ATLAS, J. High Energy Phys. 09 (2015) 049, arXiv:1503.03709.
[59] R. Aaij, et al., LHCb, J. High Energy Phys. 11 (2015) 190, arXiv:1509.07645.
[60] S. Chatrchyan, et al., CMS, Phys. Rev. D 84 (2011) 112002, arXiv:1110.2682.
[61] C. Patrignani, et al., Particle Data Group, Chin. Phys. C 40 (2016) 100001.